Theoretical investigations into the influence of the position of a breaking line on the tensile failure of flat, round, bevel-edged tablets using finite element methodology (FEM) and its practical relevance for industrial tablet strength testing

Fridrun Podczeck*, J Michael Newton, Paul Fromme

University College London, Dept. Mechanical Engineering, Torrington Place, London WC1E 7JE, UK.

*Correspondence; e-mail: f.podczeck@ucl.ac.uk; Tel +44 (0)20 7679 7178; Fax +44 (0)20 7388 0180

ABSTRACT

Flat, round tablets may have a breaking (“score”) line. Pharmacopoeial tablet breaking load tests are diametral in their design, and industrially used breaking load testers often have automatic tablet feeding systems, which position the tablets between the loading platens of the machine with the breaking lines in random orientation to the applied load. The aim of this work was to ascertain the influence of the position of the breaking line in a diametral compression test using Finite Element Methodology (FEM) and to compare the theoretical results with practical findings using commercially produced bevel-edged, scored tablets. Breaking line test positions at an angle of 0°, 22.5°, 45°, 67.5° and 90° relative to the loading plane were studied. FEM results obtained for fully elastic and elasto-plastic tablets were fairly similar, but they highlighted large differences in stress distributions depending on the position of the breaking line. The stress values at failure were predicted to be similar for tablets tested at an angle of 45° or above, whereas at lower test angles the predicted breaking loads were up to 3 times larger. The stress distributions suggested that not all breaking line angles would result in clean tensile failure. Practical results, however, did not confirm the differences in the predicted breaking loads, but they confirmed differences in the way tablets broke. The results suggest that it is not advisable to convert breaking loads obtained on scored tablets into tablet tensile strength values, and comparisons between different tablets or batches should carefully consider the orientation of the breaking line with respect to the loading plane, as the failure mechanisms appear to vary.

Keywords: Bevel-edge; Brazilian equation; Breaking line; Diametral compression test; Finite Element Method (FEM); Tablet tensile failure;

1. Introduction

Flat, round tablets usually have bevel-edges to reduce chipping of the tablet edges during packaging, transport and handling, and very often they carry a breaking ("score") line. The provision of a breaking line is an attempt to reduce the number of tablet dosing strengths required to cover a range of dosing options for a drug. At the same time, breaking lines might help patients who have swallowing difficulties and provide some flexibility in the amount of drug taken in a single dose (van Santen et al., 2002). However, as noted in the USP monograph on testing tablet breaking forces (Method 1217, USP38/NF33, 2014) the presence of a breaking line might influence the breaking forces recorded, and they hence advise that during the standard diametral compression test the orientation of the breaking line should be kept constant, either horizontally or vertically. However, in line with fracture mechanics knowledge Newton et al. (1977) recommended that the breaking line should be positioned perpendicular to the platen surfaces i.e. be parallel to the direction of loading to increase the chance of tensile failure to occur along the breaking line. As an alternative to the diametral compression test, Sovány et al. (2010) used a three-point bending test, whereby the breaking line was positioned below the upper, slightly blunted loading edge, presumably facing downward (this is not clearly specified in their paper). The advantage of a three-point bending test over the diametral compression test is that the bending moment increases linearly from zero at either support of the tablet to a maximum value at the mid-span location, and assuming linear elastic behaviour, shear effects will not affect the maximum tensile stress developing at the lower tablet surface (Stanley, 2001). Mazel et al. (2014) also suggested that for pharmaceutical compacts the three-point bending test should be preferred over the diametral compression test, because it reflects the tensile failure stress more accurately. However, this test is more sensitive to a variety of factors associated with misalignment, as well as tablet internal and surface structure (Podczeck, 2012). The flexural bending test will only provide controlled failure patterns and thus meaningful results, if the upper loading edge and the breaking line are parallel and aligned exactly below each other, and the breaking line faces downward. In this case, the bending stress will be concentrated at the tip of the breaking line and will result in, often catastrophic, failure in line with linear elastic fracture mechanics principles. In fact, a breaking load obtained with this test configuration on a tablet having a score line with a 90° opening angle could be used to determine the critical stress intensity factor of that tablet (Dunn et al., 1977). However, while bending tests are regarded as fairly simple, this would require a manual positioning of each tablet into a bending rig, which is not normally standard part of tablet breaking strength testers used in, for example, the pharmaceutical industry. Currently, pharmacopoeial breaking load tests for flat, round tablets (e.g., USP38/NF33, 2014; EP 8, 2013) are diametral in their design, and most industrially used breaking load testers have automatic tablet feeding systems, which position the tablets between the loading platens of the machine. As a result, breaking lines will be positioned with a random orientation to the applied load. In this paper only symmetric circular (round) tablets are considered. This means that the breaking line can be positioned at any angle between 0° and 90° relative to the loaded diameter. Newton et al. (1977) investigated the influence of a breaking line, which was either positioned horizontally (90°) or vertically (0°) to the loaded diameter, using photoelasticity measurements. They found that the effect of the breaking line position depended on its depth, and that for depths in the range of commercial tablet designs a horizontal breaking line position resulted in compressive stresses at the tip of the breaking line, associated with an increase in tensile stresses at the plane face. A vertical position, however, led to an increase in tensile stresses at the tip of the breaking line, associated with a reduction in the tensile stresses at the flat face. The latter would have been expected in line with linear elastic fracture mechanics, which predicts a stress concentration at the tip of a crack and reduced stresses further away from the crack (Irwin, 1957).

The aim of this work was to ascertain the influence of the position of the breaking line in a diametral compression test using Finite Element Methodology (FEM) and to compare the theoretical results with practical findings using commercially produced round, bevel-edged, scored tablets. In the FEM-work comparisons were made between flat tablets, bevel-edged tablets and bevel-edged tablets with a breaking line, whereby initially the tablet thickness (W) to diameter (D) ratio was kept constant at $W/D=0.2$ to minimise the effect of tablet thickness on the tensile stresses in the Brazilian test (Yu et al., 2006; Podczeck et al., 2013). The breaking line positions relative to the loading plane tested were 0°, 22.5°, 45°, 67.5° and 90°. In the practical experiments, similar breaking line positions were tested using diametral compression, and FEM-work was extended to include tablet dimensions matching those used in these experiments ($W/D=0.286$).

2. Materials and Methods

2.1. Software

Standard finite element methodology (FEM) was employed (Abaqus 6.12.3, Dassault Systèmes, Vélizy-Villacoublay, France). Cubic-spline interpolations were made using a Microsoft®-approved add-on to Excel 2007 (SRS1 Software, Boston, MA).

2.2. FEM model description

The basic terminology used for flat, round, bevel-edged tablets is shown in Fig. 1a. A 3D FEM model was employed to study tablets under diametral loading. For flat tablets, thickness (W) to diameter (D) ratios between 0.06 and 1.0 were compared, for bevel-edged tablets ratios between 0.2 and 0.4 were considered, and for bevel-edged tablets with breaking line ratios of W/D=0.2 and 0.286 were investigated (tablet diameter $D=0.05$ m). Comparisons were made between (a) fully flat and bevel-edged tablets, (b) bevel-edged tablets with different cup depth to tablet thickness ratio (C/W; see Fig. 1a), and (c) between bevel-edged tablets having a breaking line at different positions during loading i.e. breaking line positions tested were 0°, 22.5°, 45°, 67.5° and 90°. The bevel angle was set to α = 30° in line with standard punch design (Bauer-Brandl, 2013), and a cup depth C between 5 and 25% of the total tablet thickness W was applied to accentuate any effect of the bevel edge on the stress distributions. For tablets with breaking line a cup depth C of 25% of the total tablet thickness W was employed, as in this way, the depth of the breaking line matched the second largest depth tested in the photoelasticity models (Newton et al., 1977) and therefore allowed direct comparison of the influence of the breaking line on the stress distributions, although Newton et al. (1977) used plane-faced rather than bevel-edged tablets. Only single breaking lines with an opening angle of 90° and a depth matching the bevel were investigated.

Since the position of the breaking line results in unsymmetrical test configurations, complete tablets were modelled, positioned between two stainless steel blocks ($l=w=0.05$ m, $h=0.01$ m), similar to standard tablet breaking load testers (Fig. 1b). Boundary conditions were applied to the steel blocks to avoid tilting, slipping, sliding or twisting and only to permit movements parallel with the loading plane. To hold the tablets in place and to avoid large localised penetrations of the tablets, a surface-to-surface discretization approach was used and a friction coefficient between steel blocks and tablet surface of $\mu=0.1$ was assumed. Surface smoothing was applied to the circumferential tablet surface to avoid the need of matching nodes across the contact interface and an iterative solver algorithm was chosen. 3D-quadratic tetrahedral elements were used for the meshing. The mesh density to achieve a stable and accurate solution was optimised using a convergence test as described earlier (Podczeck et al., 2013). The mesh density of the blocks ($s=0.002$) was kept slightly below that of the tablets ($s=0.0011$) to ensure convergence.

The stainless steel blocks were modelled from engineering steel with a Young's modulus of 209 GPa and a Poisson's ratio of 0.3. The load P was transmitted through both blocks (i.e. $P/2$ per block) to prevent unsymmetrical loading and distortions. As in previous work (Podczeck et al., 2013) and as used by others (Pitt et al., 1989) the load P was calculated as 100N mm^{-1} of total tablet thickness to maintain a standard load intensity. For the tablets only one linear elastic model with the properties of Araldite CT200, hardened with 30% w/w Hardener 901, for which Young's modulus of elasticity (2.58 GPa) and Poisson's ratio (0.35) were taken from the literature (Burger, 1969), was studied. This model was chosen to enable a direct comparison with the photoelasticity results reported by Newton et al. (1977). The theory of elasticity (Timoshenko and Goodier, 1987) predicts that relative stress distributions are independent of Young's modulus and Poisson's ratio, and that this holds in FEM studies has previously been confirmed (Pitt and Heasley, 2013, Podczeck et al., 2013). There is therefore no need to repeat the analyses with other elasticity data. An elasto-plastic model with similar Young's modulus and Poisson's ratio as above plus a yield strength of 25.8 MPa at a plastic strain of 0.01 was also tested to reflect maximum underestimation of the failure stress (Procopio et al., 2003). To ensure convergence, in the elasto-plastic models the initial step time and step increment size were slightly reduced.

2.3. Practical work

Bevel-edged, scored tablets were purchased to be able to reflect the larger variability of tablet breaking loads of commercially produced compacts during testing: (1) Superdrug Diarrhoea Relief Tablets (SDRT), Surepharm Services Ltd., Burton-Upon-Trent, UK, batches 4A058 and 3J114; (2) Aspirin 300 mg Dispersible Tablets (ADT), Boots Company PLC, Nottingham, UK, batch 140032.

The main ingredients of the SDRT tablets are 400 mg light kaolin and 75 mg calcium carbonate. The remaining excipients are icing sugar, maize starch, magnesium stearate, erythrosine, clove-, cinnamon- and nutmeg oil. The estimated powder particle density of the mixture is 2150 kg m^{-3}. The ADT tablets contain 300 mg of acetylsalicylic acid, plus lactose, sodium saccharin, maize starch, citric acid, sodium lauryl sulphate, talc and calcium carbonate as excipients. The estimated powder particle density of the mixture is 1400 kg m^{-3}.

The breaking load of the tablets was determined using a CT6 tablet strength tester (Engineering Systems, Nottingham, UK), equipped with a 50 kg load cell, at a test speed of 1 mm min^{-1}. The breaking load was recorded with an accuracy of ±0.005 kg. The tester was linked to a laptop (Dell Latitude D505, Dell UK, Bracknell, Berkshire) via a USB cable. Machine inherent plotter software (Graph Plotter®, V2.09; Engineering Systems, Nottingham, UK) was installed and used to control the tester remotely from the computer. Force versus displacement curves were recorded for each tablet using a recording frequency of 1000 Hz. They were exported into

Windows Excel 2007 (Microsoft®) and further processed to obtain the slope of the linear portion of the force-displacement curves.

Tablets were weighed to ±0.001 g (Sartorius BP 121S, Göttingen, Germany) and their dimensions were measured to ±0.001 mm (Moore and Wright MED961D Digital Micrometer, Neill Tools Ltd., Sheffield, UK). A protractor was used to mark the exact test positions for the tablets to be placed between the loading platens of the CT6.

To determine the exact cup depth and width of the breaking line, photographs (Olympus SP-500UZ, Olympus Imaging Corp., Hamburg, Germany) of the tablets were taken with a magnification of x50 (diameter view) and x100 (thickness view) against a graticule (Graticule Ltd., Tonbridge, UK).

2.4. Statistical analysis

Analysis of Variance (ANOVA) was performed using SPSS 20.0 (SPSS-IBM, Woking, UK). The post-hoc Scheffé test (Scheffé, 1959; Berry and Lindgren, 1996) was used for multiple comparisons to identify significantly different samples and sample groups. The level of significance (α-error) was set to $p=0.05$ in all cases.

3. Results and Discussion

3.1. FEM analysis of elastic discs

The tablet thickness (W) to diameter (D) ratio affects the applicability of the Brazilian equation (Barcellos, 1953; Carneiro, 1953; Fell and Newton, 1968, 1970), which had been developed strictly in a two-dimensional space. Yu et al. (2006) recommended that for *W/D*-ratios above 0.5 a correction of the tensile failure stress should be applied, but Podczeck et al. (2013) indicated that this might already be required for lower *W/D*-ratios. Hence, flat tablets with *W/D*-ratios between 0.06 and 1.0 were modelled and the deviations of the tensile stress at the tablet centre (coordinates $x=y=z=0$) and the outer cylinder surface (coordinates $x=y=0$; $z/W=1$) from the 2D-solution are shown in Fig. 2. As can be seen from the figure, deviations from the theoretical tensile failure stress are already present at a *W/D*-ratio of 0.1.

Bevel edges of 5, 10, 15, 20 and 25% of the total thickness of the flat discs were added for discs with a *W/D*-ratio of 0.2, 0.3 and 0.4. These, however, did not significantly affect the stress distributions (see below) and reduced the tensile stresses in the centre and at the surface of the discs by less than 1% in all cases. It was hence decided to use a *W/D*-ratio of 0.2 for the work comparing the influence of the position of the breaking line, as here the deviations from the Brazilian solution appeared still reasonably small (1.6% in the centre and 2.5% at the surface of the disc; Fig. 2). A cup depth of 25% of the total tablet thickness was used to accentuate any potential contribution of the bevel edge on the stress distributions.

For post-processing of the results, the x-axial stress distributions were first studied graphically using an inverse rainbow colour scheme with 2 MPa and 0 MPa as maximum and minimum threshold levels. Hence, maximum tensile stresses are coloured dark blue, whereas compressive stresses are red in all figures. Various views and cuts were produced in all three dimensions of space to investigate the stress distribution changes throughout the discs. Secondly, the numeric values along the z-axis were collected and compared to get a better assessment of the magnitude of x-axial stresses inside the discs.

As stated above, in order to determine the influence of the bevel edge on the stress distribution, a flat and a bevel-edged disc were compared. From Fig. 3a it can be seen that the bevel edge only slightly affects the stress distributions at the front, centre or rear of the discs in the XY-plane. In the centre the tensile stresses at the surface of the discs seem to be lower when a bevel edge is present, and at the outer surfaces the tensile stresses are slightly less pointed and broader in this case. The average tensile stress across the z-axis, however, is only reduced by 0.6% despite the accentuated cup depth of 25% of the tablet thickness, compared to the flat disc, and this reduction is consistent across the whole failure plane. Nevertheless, when comparing the discs with breaking lines, the numerical x-axial stress values were normalised using the x-axial stress values obtained from the bevel-edged disc to avoid propagation of stress deviations.

In Fig. 3b the x-axial stress distributions are compared in the YZ- and XZ-planes, whereby the YZ-plane is equal to the failure plane, assuming tensile failure of the discs. Again comparing the flat with the bevel-edged tablet, it can be seen that in the XZ-plane there is no difference in stress distribution. In the YZ-plane i.e. failure plane the differences are marginal. An important practical consequence of the comparison of the stress distributions between flat and bevel-edged discs is the applicability of the Brazilian equation (Barcellos, 1953; Carneiro, 1953; Fell and Newton, 1968, 1970) to calculate a tablet tensile strength from a diametral compression test with or without correction, depending on the *W/D*-ratio, regardless of whether a tablet has been furnished with a bevel edge or not, provided failure occurred in tension and without larger deformation underneath the loading points, as previously suggested (Podczeck, 2012).

If the breaking line is positioned at a 0°-angle to the loading direction, then in line with linear elastic fracture mechanics a stress concentration at the tip of the crack can be observed (Fig. 3a,b). Consequently, the centrally observed tensile stresses are increasingly reduced the further away they are observed from the tip of the breaking line and are smallest at the rear of the tablet. This can be clearly seen in all three planes (XY, Fig. 3a; YZ and XZ, Fig. 3b). This suggests that these tablets will fail in tension, but the failure will be initiated at the tip of the breaking line and will travel across the YZ-plane through its centre to the rear side of the tablet. In contrast, for flat tablets it had been proposed that failure is initiated at both outer tablet surfaces simultaneously and travels towards the tablet centre along the YZ-plane at which point tensile failure will occur (Yu et al., 2006).

If the breaking line is turned to the 22.5° loading position, there is still a considerable stress concentration in the centre of the breaking line, but in addition there is also some broad area of tensile stresses closely underneath the loading points (Fig. 3a). Also here, the reduction of tensile stresses towards the rear of the tablet can be observed, but this effect is slightly less when compared with the 0°-position (Fig 3b). A possible breaking pattern might hence be the start of crack propagation in the centre of the breaking line with failure moving towards the rear of the tablet, but at the same time breaking might be initiated underneath the loading platens potentially leading to some deviation from a clean tensile failure across the YZ-plane.

At a 45° angle of the breaking line a very different picture emerges. At the front of the disc (Fig. 3a) tensile stresses are concentrated along the loading diameter with a slight disruption in the centre of the disc inside the breaking line. In the centre of the tablet along the XY-plane tensile stresses are much lower, but follow more or less the breaking line position, and this is even more apparent at the rear of the disc, where the tensile stresses are highest opposite the breaking line and underneath the loading points. First of all this indicates a conversion to the stress pattern observed on the simple bevel-edged disc suggesting that failure will be initiated from the periphery of the disc on either side and might not be too dissimilar in the final failure load. On the other hand, the stress distribution in the YZ-plane still shows a small stress concentration at the tip of the crack (Fig. 3b) and some asymmetric stress distribution across the XZ-plane, the consequences of which can only be identified using practical experiments (see section 3.3).

When the disc is turned further to 67.5° and ultimately to 90°, tensile stresses inside the breaking line are replaced by compressive stresses (Fig. 3a), in particular for the 90° test position (Fig. 3b). If failure is initiated by the tensile stresses underneath the loading platens, these discs could still fail in tension, but especially in the 90° position the large compressive stresses seen in the XZ-plane (Fig. 3b) could also indicate a collapse or folding of the disc along the breaking line during loading. Again, which mechanism will apply cannot be derived from the FEM results and requires practical assessment (see section 3.3).

In Fig. 4 the normalised x-axial stresses along the z-axis are compared (a negative sign indicates compressive, while a positive sign indicates tensile stress). For the 0° and the 90° angle these are in very good agreement with the findings reported employing photoelasticity work (Newton et al., 1977). As observed in the photoelasticity work, the compressive stresses along the breaking line at the 90° test position are again accompanied by an increase in tensile stresses at the opposite tablet face, when compared to the standard bevelled disc, and the FEM work now allows to extend this observation to the 67.5° test position. On the other hand, at the 0° and 22.5° test positions there is a clear and large stress concentration at the tip of the crack and stresses initially drop quickly and then more gradually towards the other tablet face. Failure should in these cases thus be initiated at the tip of the breaking line. In the 45° test position the normalised stresses are only slightly but consistently larger than those observed on the bevel-edged disc, and the largest and similar stress values are observed at the opposite face and at a point ½ the depth of the breaking line towards the centre of the disc. These might be the positions where crack propagation across the YZ-plane will be simultaneously initiated most likely leading to tensile failure of the tablet.

If the absolute maximum tensile stresses are plotted as a function of the angle of the breaking line test position (Fig. 5), it can be seen that the failure values should be similar for tablets tested at an angle of 45° or above, whereas at lower test angles the breaking loads might be up to 3 times larger, provided that the tablets fail in tension. In practice this would mean that under automatic test conditions provided by modern strength testers used in the pharmaceutical industry a larger variability in the breaking loads would be observed, unless the testers were equipped with a sorting mechanism ensuring that either all tablets are positioned with a breaking line position of 0° (preferred due to proposed failure mechanism), or that the breaking line is randomly positioned between 45° and 90° to reduce variability whereby neglecting the changes in the failure mechanism. In any case, however, the failure loads and the breaking mechanisms do not satisfy the criteria imposed by the Brazilian equation (Barcellos, 1953; Carneiro, 1953; Fell and Newton, 1968, 1970; Podczeck, 2012) and a conversion into a tablet tensile stress should be avoided.

3.2. FEM analysis of elasto-plastic discs

According to Procopio et al. (2003) the Brazilian equation underestimates the true failure stresses if the tablets behave elasto-plastic under load. This could apply mainly to tablets containing larger amounts of ductile excipients such as microcrystalline cellulose, cellulose ethers and other polymeric excipients such as polyvinyl pyrrolidone or xanthan gum. The above described FEM analysis was hence repeated for an elasto-plastic material, whereby the material properties were chosen to simulate maximum underestimation as identified by Procopio et al. (2003). Similar model values had also been used in the FEM evaluation of doubly-convex discs (Podczeck et al., 2013).

In Fig. 6a,b as before, the x-axial stresses are compared in the XY- (Fig. 6a), and the YZ- and XZ-planes (Fig. 6b). Only marginal differences in the stress distributions can be identified when comparing the elasto-plastic (Fig. 6a,b) with the elastic model figures (Fig. 3a,b). For example, for the bevel-edged disc in the elasto-plastic model there are still some large tensile stresses (blue areas) underneath the loading points in the centre of the disc. On average the stresses along the z-axis in the elasto-plastic flat disc compared to the elastic flat disc are reduced only by 0.5±0.2 %, but in the bevel-edged elasto-plastic disc stress reductions of 3.0±0.2 % are seen. The largest reductions in the absolute stress values along the z-axes for elasto-plastic discs are found for the 0° and 67.5° test angles (4.6±4.3% and 4.5±4.9 %, respectively), and these are also highly variable. For the 0° test angle the reduction in stress values increases from the tip of the crack (0.7 %) towards the opposite face (13.3 %), and this is best seen in Fig. 6b, YZ-plane, where yellow colour emerges at the flat surface opposite the breaking line. For the 67.5° test angle, the largest reduction (16.7 %) is found at a point ½ the depth of the breaking line towards the centre of the disc, whereas the smallest reduction is observed directly at the tip of the crack (0.6 %). This can also be seen in Fig. 6b, XZ-plane, where the red spot underneath the crack represents tensile stresses close to zero. Average reductions of 2.6±0.2 % and 2.7±0.2 %, when compared with the fully elastic discs, are obtained for elasto-plastic discs with test angles of 22.5° and 45°, respectively. For the 45° test angle this cannot be observed in the pictures, but for the 22.5° test position the changes are visualised in the XZ-plane (Fig. 3b vs. 6b). The smallest average reduction is found for the 90° test position (0.3 %), but due to a large decrease in the compressive stresses at a point ½ the depth of the breaking line towards the centre of the disc of almost 70 % the variability of this reduction is large (36.1 %). This can also be observed when comparing the pictures in the XY-planes (Fig. 3a vs. 6a), where larger blue tensile areas and broader green tensile areas are visible for the elasto-plastic disc.

The normalised x-axial stresses along the z-axis developing in elasto-plastic discs (Fig. 7a; a negative sign indicates compressive, whereas a positive sign indicates tensile stress) are very similar to those seen when stressing fully elastic discs (Fig. 4). This is not surprising considering the loading technique used in this paper. Procopio et al. (2003) enforced a vertical displacement of up to 10% of the original tablet diameter in order to overcome the yield strength of their model discs, which resulted in tensile stresses of 20 MPa and more. Pharmaceutical tablets, however, typically fail at tensile stresses between 1 and 5 MPa. In this work, loading with a defined pressure (1.273 MPa for discs with $W/D=0.2$) was hence preferred. The plastic component of the elasto-plastic response of the discs to the applied load will hence be very small, and differences as large as those observed by Procopio et al. (2003) cannot be expected. As before, the compressive stresses along the breaking line at the 90° and 67.5° test positions are accompanied by an increase in tensile stresses at the opposite tablet face, when compared to the standard bevelled disc. At the 0° and 22.5° test positions there is again a clear and large stress concentration at the tip of the crack and stresses initially drop quickly and then more gradually towards the other tablet face indicating that failure should be initiated at the tip of the breaking line. In the 45° test position the normalised stresses are, as for fully elastic discs, only slightly but consistently larger than those observed on the bevel-edged disc, and again the largest and similar stress values are observed at the opposite face and at a point ½ the depth of the breaking line towards the centre of the disc. The largest difference between an elastic and an elasto-plastic disc can be seen, when the von Mises stresses of a disc in the 90° test position are compared (Fig. 7b). These differences are mainly in the vicinity of the breaking line and indicate that deformation will first occur here rather than in the bulk of the tablet.

If the absolute maximum tensile stresses are plotted as a function of the angle of the breaking line test position (Fig. 5), similarly to fully elastic discs failure values should be similar for tablets tested at an angle of 45° or above, whereas at lower test angles the breaking loads might be up to 3 times larger, provided that the tablets fail in tension.

3.3. Experimental assessment of the failure properties of scored tablets

Table 1 summarises the tablet properties observed. As these tablets were manufactured under industrial conditions, their weights and thicknesses are variable. Batch 3J114 of the Diarrhoea Relief Tablets is heavier yet the tablets are thinner than those of batch 4A058, and hence their estimated porosity is slightly less. The Aspirin Tablets are soluble tablets and therefore highly porous.

FEM work (see section 3.2.) did predict that tablets tested at a 0° angle of the breaking line position with respect to the loading plane would result in up to 3 times stronger tablets and that tablets tested at angles between 45 and 90° would be similar and weakest. A trend that test angles below 45° result in stronger tablets can only be observed for Diarrhoea Relief Tablets, batch 3J114, but this is most likely a random occurrence without practical significance. Analysis of Variance was performed for all three tablet batches, each time comparing the breaking loads obtained at the various test angles. The Levene test was in all cases statistically not significant ($p > 0.99$) demonstrating homogeneity of variance, and all overall F-tests were equally statistically not significant ($p > 0.01$ for all three tablet batches). The Scheffé test was also unable to separate different batches. The large differences predicted by FEM analysis hence appear of no relevance in practice, if only breaking loads are considered.

However, it is important to remember that even breaking loads should only be compared between tablet batches, if the failure mechanisms are the same (Fell and Newton, 1970). To assess the failure mechanisms for different loading angles, initially force-displacement curves were recorded during tablet testing. These were all linear over more than 90 % of their total length, and hence the slopes were calculated for all tablets. For Diarrhoea Relief Tablet batch 4A058 the slopes ranged from 22.1 ± 2.3 N μm^{-1} (90°) to 22.9 ± 1.0 N μm^{-1} (67.5°); for batch 3J114 they ranged from 24.6 ± 0.8 N μm^{-1} (67.5°) to 27.0 ± 1.3 N μm^{-1} (22.5°); and for Aspirin tablets they ranged from 23.3 ± 1.0 N μm^{-1} (45°) to 23.8 ± 1.7 N μm^{-1} (0°). The slopes seem only to be related to the overall breaking load and the type of tablet, but they are not related to the angle of the breaking line during the test. The only physical property of the tablets that can be inferred from the linearity of the slopes is that all tablets failed by unstable crack propagation indicating that sufficient energy had developed to propagate the most suitably orientated flaw inside the tablets suddenly and completely across the failure plane. This is typical of elastic behaviour of brittle specimen (Adams, 1985).

Despite the generally similar fracture mechanism identified from the force-displacement curves, there are subtle differences in the crack initiation. Fig. 8 shows this for all five test angles as observed for Diarrhoea Relief Tablets batch 4A058. If the breaking line is positioned at 0° to the loading plane, then the crack appears to initiate at the centre of the tablet and follows the breaking line (Fig. 8a), which is in line with the FEM observations. If the breaking line is positioned 22.5° to the loading plane, then crack propagation potentially starts at the centre and inside the breaking line (Fig. 8b, left), but the majority of tablets showed patterns where crack propagation started simultaneously in the centre along the breaking line and underneath the loading points (Fig. 8b, right). Again this is in agreement with the FEM predictions discussed above. At an angle of 45° again in some cases fracture appears to initiate at the centre of the tablets inside the breaking line (Fig. 8c, left), but on the whole tablets seem to break into two halves, although the failure line is not ideally straight and smooth, and there is a shift of the breaking line in the centre of the tablets (Fig. 8c, right). This again matches FEM observations. A similar observation is made for a test angle of 67.5° (Fig. 8d), but here in the centre of the tablet the fracture line follows the breaking line more closely (Fig. 8d, right). Finally, when the breaking line is positioned 90° towards the loading direction, the tablets appear to fail in tension (Fig. 8e). Hence the compressive forces seen in the FEM analysis do not lead to folding and tablet collapse during testing.

As the predicted differences in the breaking load of the tablets as a function of the angle between breaking line and loading plane could not be found in the practical experiments, elastic discs with relative dimensions similar to the Diarrhoea Relief Tablets, namely *W/D*=0.286 and cup depth of 14.4% of the total tablet thickness, were reproduced for further FEM-testing. Table 2 compares the stress values and the resulting factors for the stress values at the centre of the discs and the maximum tensile stress values, comparing all three FEM-models used (viz. elastic, elasto-plastic, elastic with relative tablet dimensions matching those of the Diarrhoea Relief Tablets). As can be seen, if the maximum tensile stress in the failure plane were responsible for the breaking load that would be measured (Pitt et al., 1989) then the ratio between the failure loads of a tablet with the breaking line positioned at an angle of 0° to the loading plane and that of a 90° position would be 2.8 regardless of the model used and the relative dimensions of the bevel-edge and the breaking line. If tablet failure was initiated at the centre of the tablets, which according to Peltier (1954) is an essential prerequisite for valid tensile failure, then the factor i.e. the ratio between the failure loads of a tablet with the breaking line positioned at an angle of 0° to the loading plane and that of a 90° position would be 1.3 for a tablet of the dimensions of the Diarrhoea Relief Tablets. This would still mean that there should be a difference of 15 N in the breaking load of the experimentally tested tablets, which is not the case (see Table 1). Large discrepancies between FEM-predictions and experimental data have previously been noted for simple flat-faced tablets (Ehrnford, 1980, 1981), and Darvell (1990) concluded that “finite element analysis can only be as good as the theory used to make the calculations, and the theory is at present insufficiently worked out”. While the theory behind FEM calculations has advanced considerably since Darvell’s statement, for bevel-edged tablets with a breaking line there is no analytical solution available, making it difficult to identify the reasons for the discrepancies observed. For example, the porosity of the tablets will be lowest underneath the breaking line due to the highest compression stress and maximum compaction (Bauer-Brandl, 2013), resulting in nonhomogeneous and potentially non-isotropic specimen, yet all FEM-models used in this work assumed homogeneity and fully isotropic behaviour of the discs. The breaking line will be rounded at the bottom; sharp tooling would be subject to breakage during compaction. The tablet porosity, which ranged from 19 and 21% for Diarrhoea Relief Tablets to 47% for the Aspirin tablets, as well as pore size and pore shape distributions will also influence the stresses developing inside the tablets. FEM-models can be produced for porous specimens, and porosity distributions can be modelled, for example, to acknowledge the increased density beneath the breaking line, but such simulations are beyond the scope of this work.

4. Conclusions

FEM results obtained for fully elastic and elasto-plastic tablets are fairly similar in terms of the stress distributions within the tablets. However, there are large differences in stress distributions depending on the position of the breaking line. FEM predicts the stress values at failure to be similar for tablets tested at an angle of 45° or above, whereas at lower test angles the predicted breaking loads are up to 3 times larger. The stress distributions suggest that not all breaking line angles would result in clean tensile failure. In practice, however, these differences in breaking load are not found, but differences in the way tablets break can be observed. The results suggest that it is not advisable to convert breaking loads obtained on scored tablets into tablet tensile strength values, and comparisons between different tablets or batches should carefully consider the orientation of the breaking line with respect to the loading plane, as the failure mechanisms appear to vary.

Acknowledgements

The authors are grateful to Denis Cooper and Simon Carter (Engineering Systems, Nottingham, UK) for the loan of the CT6 tablet strength tester. Daniel Ashworth's help to overcome a remote access problem to the Linux server was invaluable, as was the server and software maintenance performed by David Bevan and Mark Iline (all from UCL Mechanical Engineering, UK).

References

Adams, M.J., 1985. The strength of particulate solids. J. Powder Bulk Solids Technol. 9, 15–20.

Barcellos, A., 1953. Tensile strength of concrete — correlation between tensile and compressive concrete strength. RILEM Bull. 15, 109–113.

Bauer-Brandl, A., 2013. Tooling for tableting. In: Encyclopedia of Pharmaceutical Science and Technology, 4th ed. Taylor and Francis, New York, pp. 3628–3644.

Berry, D.A., Lindgren, B.W., 1996. Statistics — Theory and Methods. 2nd ed. Duxbury Press, Belmont, pp. 577–578.

Burger, C.P., 1969. A generalized method for photoelastic studies of transient thermal stresses. Exp. Mech. 9, 529–537.

Carneiro, F.L.L., 1953. Tensile strength of concrete – a new method for determining the tensile strength of concretes. RILEM Bill. 13, 103-107.

Darvell, B.W., 1990. Uniaxial compression tests and the validity of indirect tensile strength. J. Mater. Sci. 25, 757-780.

Dunn, M.L., Suwito, W., Cunningham, S., 1997. Fracture initiation at sharp notches: correlation using critical stress intensities. Int. J. Solid Struct. 34, 3873-3883.

Ehrnford, L., 1980. The connection between load distribution and fracture load in the diametral compression test – an experimental study. Swed. Dent. J. 4, 201-212.

Ehrnford, L., 1981. Stress-distribution in diametral compression tests. Acta Odontol. Scand. 39, 55-60.

EP 8 (European Pharmacopoeia, 8th edn.), 2013. Resistance to Crushing Force (Method 2.9.8). European Directorate for the Quality of Medicines and Health Care. Strasbourg.

Fell, J.T., Newton, J.M., 1968. The tensile strength of lactose tablets. J. Pharm. Pharmacol. 20, 657-658.

Fell, J.T., Newton, J.M., 1970. Determination of tablet strength by the diametral compression test. J. Pharm. Sci. 59, 688-691.

Irwin, G.R., 1957. Analysis of stresses and strains near the end of a crack traversing a plate. J. Appl. Mech. 24, 361-364.

Mazel, V., Diarra, H., Busignies, V., Tchoreloff, P., 2014. Comparison of different failure tests for pharmaceutical tablets: Applicability of the Drucker-Prager failure criterion. Int. J. Pharm. 470, 63-69.

Newton, J.M., Stanley, P., Tan, C.S., 1977. Model study of stresses in grooved tablets under diametral compression. J. Pharm. Pharmacol. 29, 40P.

Peltier, R., 1954. Theoretical investigation of the Brazilian test. RILEM Bull. 19, 29-69.

Pitt, K.G., Newton, J.M., Stanley, P., 1989. Stress distributions in doubly convex cylindrical discs under diametral loading. J. Phys. D: Appl. Phys. 22, 1114–1127.

Pitt, K.G., Heasley, M.G., 2013. Determination of the tensile strength of elongated tablets. Powder Technol. 238, 169–175.

Podczeck, F., 2012. Methods for the practical determination of the mechanical strength of tablets — From empiricism to science. Int. J. Pharm. 436, 214–232.

Podczeck, F., Drake, K.R., Newton, J.M., 2013. Investigations into the tensile failure of doubly-convex cylindrical tablets under diametral loading using finite element methodology. Int. J. Pharm. 454, 412–424.

Procopio, A.T., Zavaliangos, A., Cunningham, J.C., 2003. Analysis of the diametral compression test and the applicability to plastically deforming materials. J. Mater. Sci. 38, 3629–3639.

Scheffé, H., 1959. The Analysis of Variance. Wiley, New York; (reprinted 1999, ISBN 0-471-34505-9).

Sovány, T., Kása, P., Pintye-Hódi, K., 2010. Modeling of subdivision of scored tablets with the application of artificial neural networks. J. Pharm. Sci. 99, 905–915.

Stanley, P., 2001. Mechanical strength testing of compacted powders. Int. J. Pharm. 227, 27–38.

Timoshenko, S.P., Goodier, J.N., 1987. Theory of Elasticity. 3rd ed. McGraw-Hill, New York.

USP38/NF33 (United States Pharmacopoeia/National Formulary), 2014. Tablet Breaking Force (Method 1217). The United States Pharmacopoeial Convention, Rockville, MD.

Van Santen, E., Barends, D.M., Frijlink, H.W., 2002. Breaking of scored tablets: a review. Eur. J. Pharm. Biopharm. 53, 139–145.

Young, L.L., 1995. Tableting Specification Manual. American Pharmaceutical Association, Washington, DC, p. 46.

Yu, Y., Yin, J., Zhong, Z., 2006. Shape effects in the Brazilian tensile strength test and a 3D FEM correction. Int. J. Rock Mech. Min. Sci. 43, 623–627.

Legends to Figures

Figure 1

Tablet modelling. (a) Basic terminology used for flat, round, bevel-edged tablets; (b) FEM model of a tablet positioned between two steel blocks during diametral compression testing; ϕ = angle between the breaking line and the loading plane; P = applied load (in Pa).

Figure 2

x-axial tensile stresses observed in flat elastic discs using FEM-modelling.

Figure 3

x-axial stress distribution in elastic discs with breaking line – (a) XY-Plane; (b) YZ and XZ-Planes.

Figure 4

Normalised x-axial stresses along the z-axis (coordinates $x=y=0$), obtained on elastic discs (the solid line at a normalised stress of 1 represent the bevel-edged disc).

Figure 5

Maximum tensile stress as a function of the angle between the breaking line and the loaded diameter of the tablet.

Figure 6

x-axial stress distribution in elasto-plastic discs with breaking line – (a) XY-Plane; (b) YZ and XZ-Planes.

Figure 7

Normalised stresses along the z-axis (coordinates $x=y=0$); (a) x-axial stresses obtained on elasto-plastic discs (the solid line at a normalised stress of 1 represents the bevel-edged disc); (b) von Mises stresses comparing elastic (solid lines) and elasto-plastic (dashed lines) discs with a 90° angle between loading plane and breaking line (the lines at a normalised stress of 1 represent the bevel-edged discs).

Figure 8

Crack initiation in Diarrhoea Relief Tablets, batch 4A058, at different breaking line positions relative to the loading diameter; (a) 0°; (b) 22.5°; (c) 45°; (d) 67.5°; (e) 90°.

Figure 1a

Basic terminology of flat, round, bevel-edged tablets (Young, 1995). *W* = tablet thickness; *B* = band thickness; *C* = cup depth; D = tablet diameter; α = bevel angle (30°).

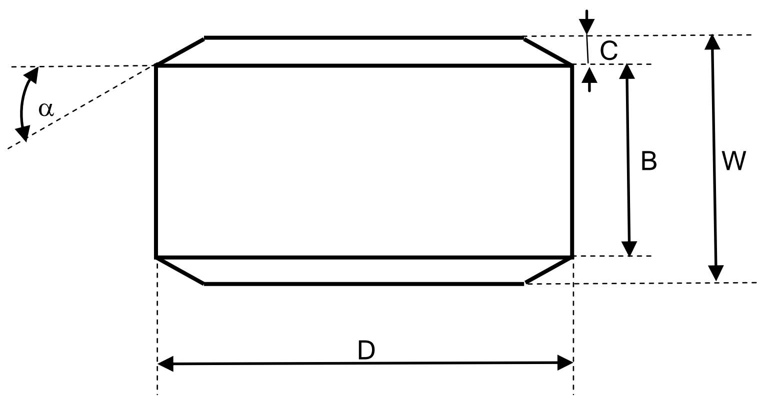

Figure 1b

FEM model of a tablet positioned between two steel blocks during diametral compression testing; ϕ = angle between the breaking line and the loading plane; P = applied load (in Pa).

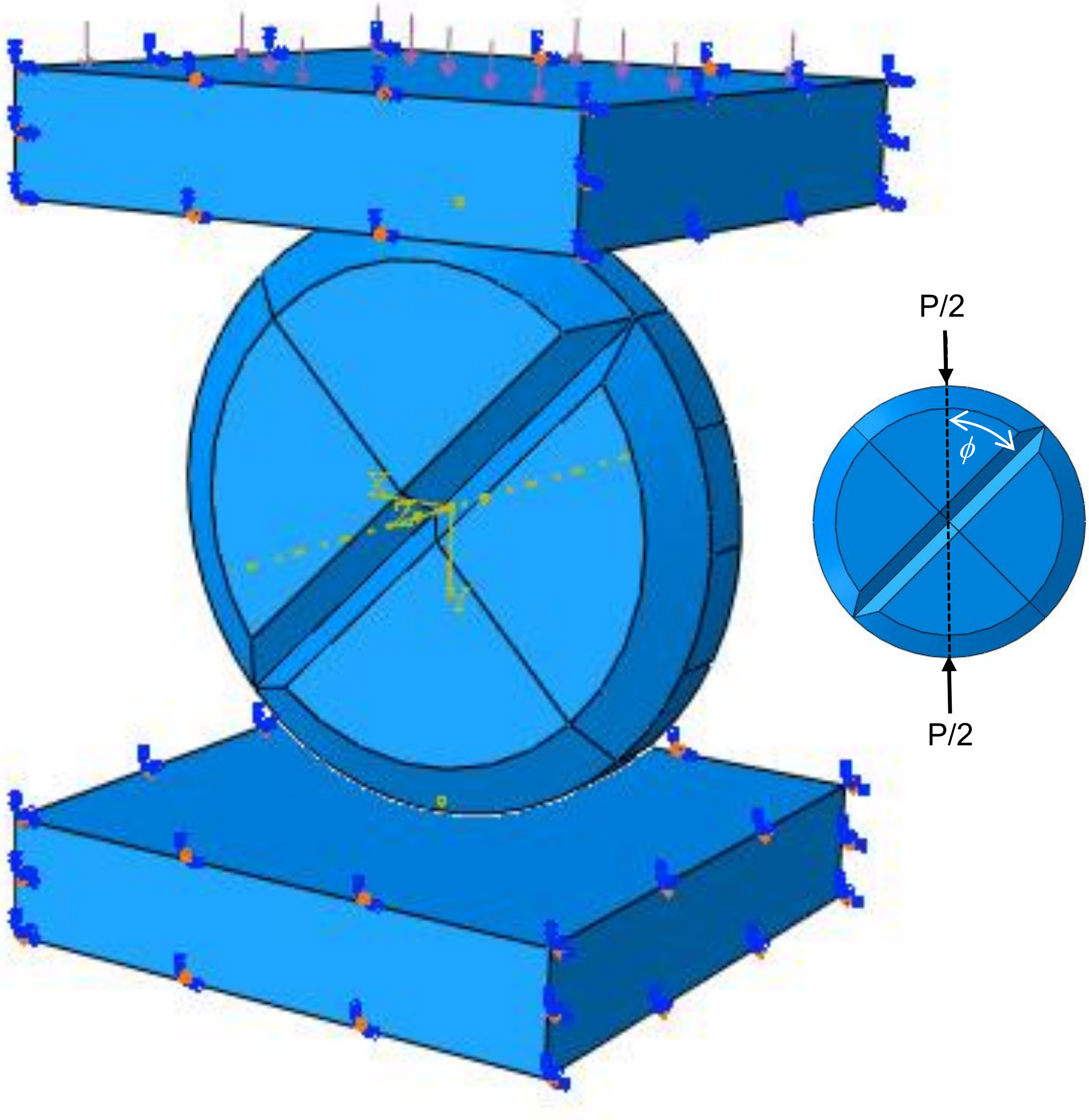

Figure 2: Tensile stresses observed in flat elastic discs using FEM-modelling.

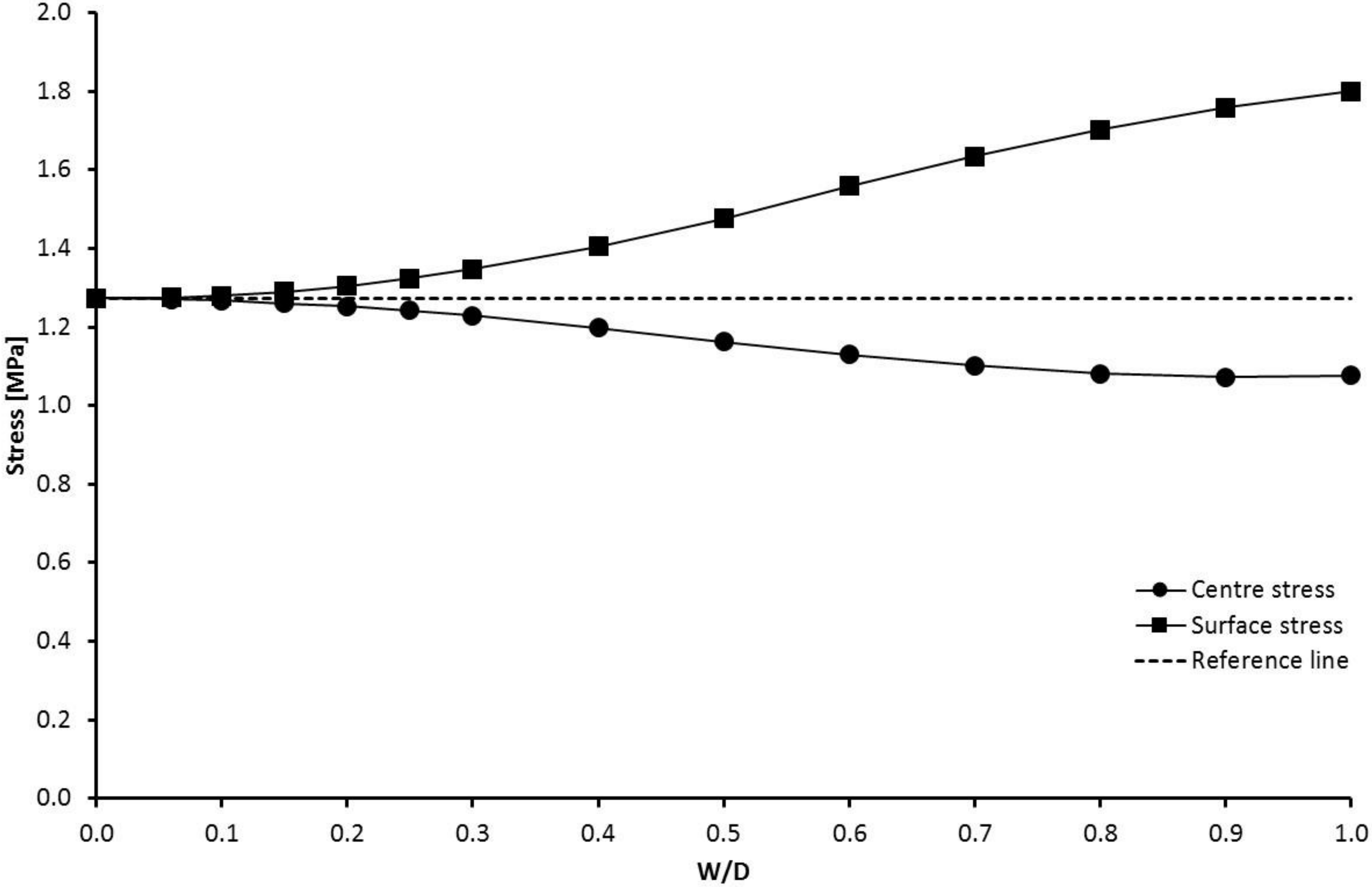

Figure 3a

Stress distribution in elastic discs with breaking line – XY-Plane.

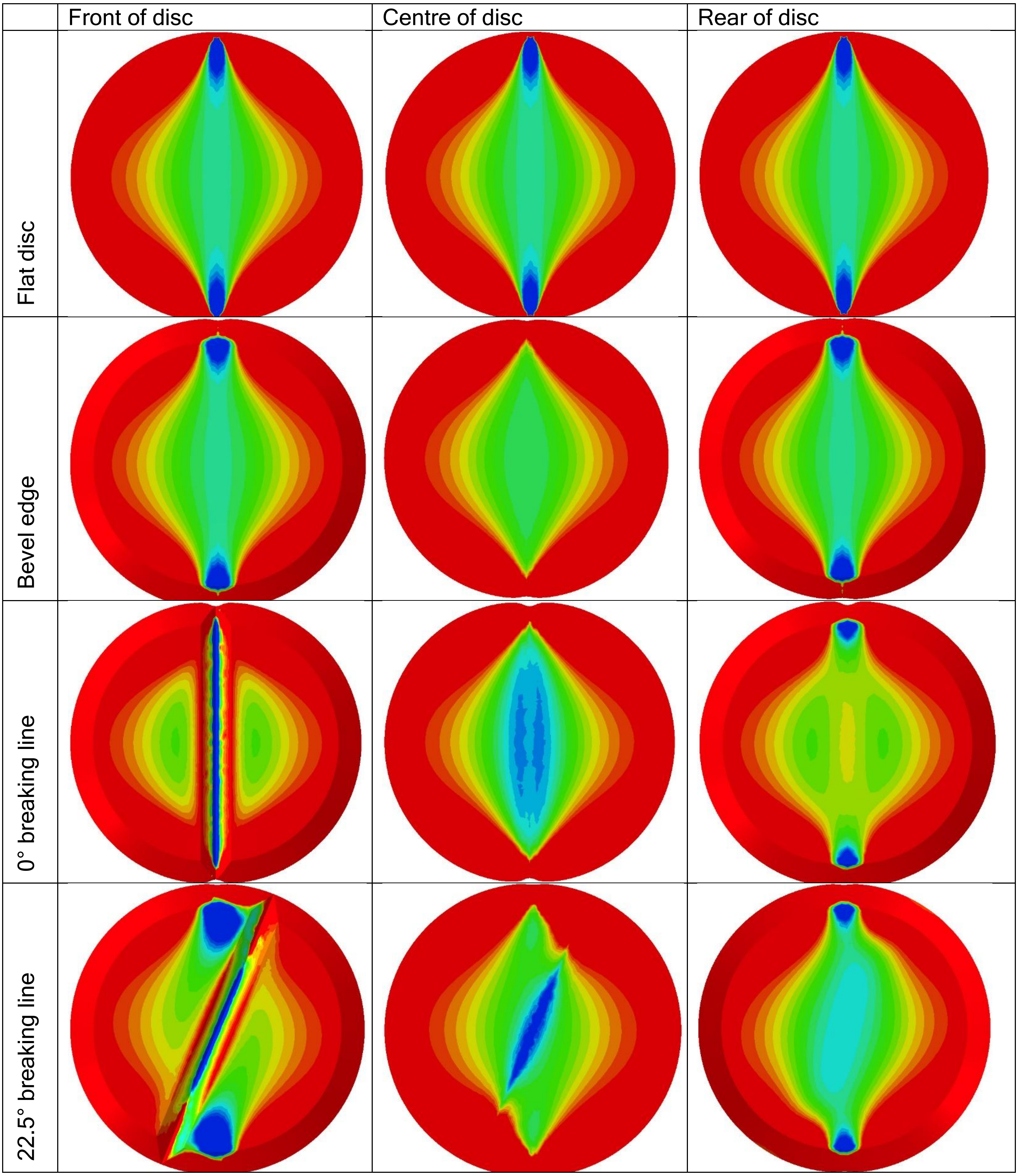

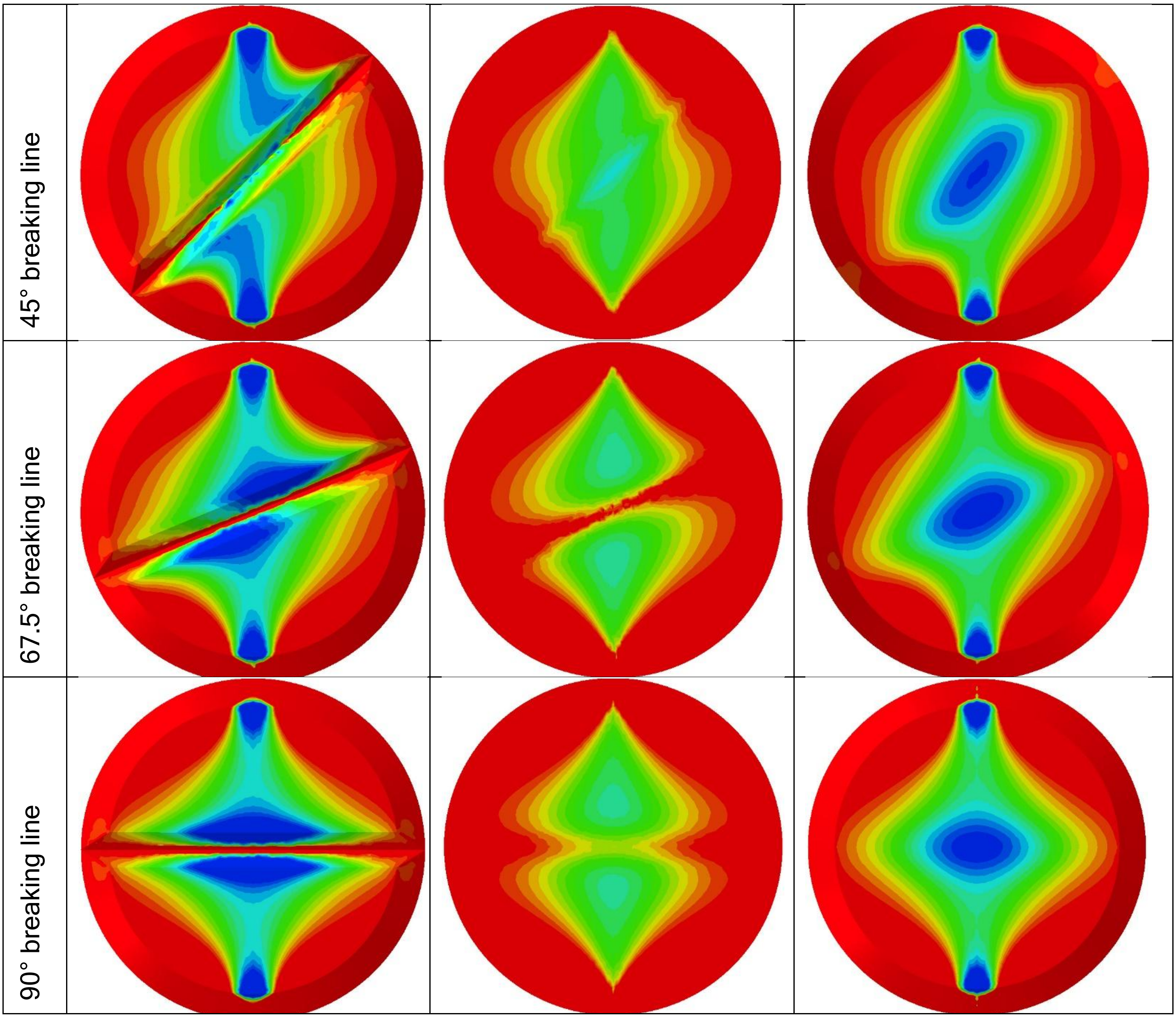

Figure 3a (continued)

Figure 3b

Stress distribution in elastic discs with breaking line – YZ and XZ-Planes.

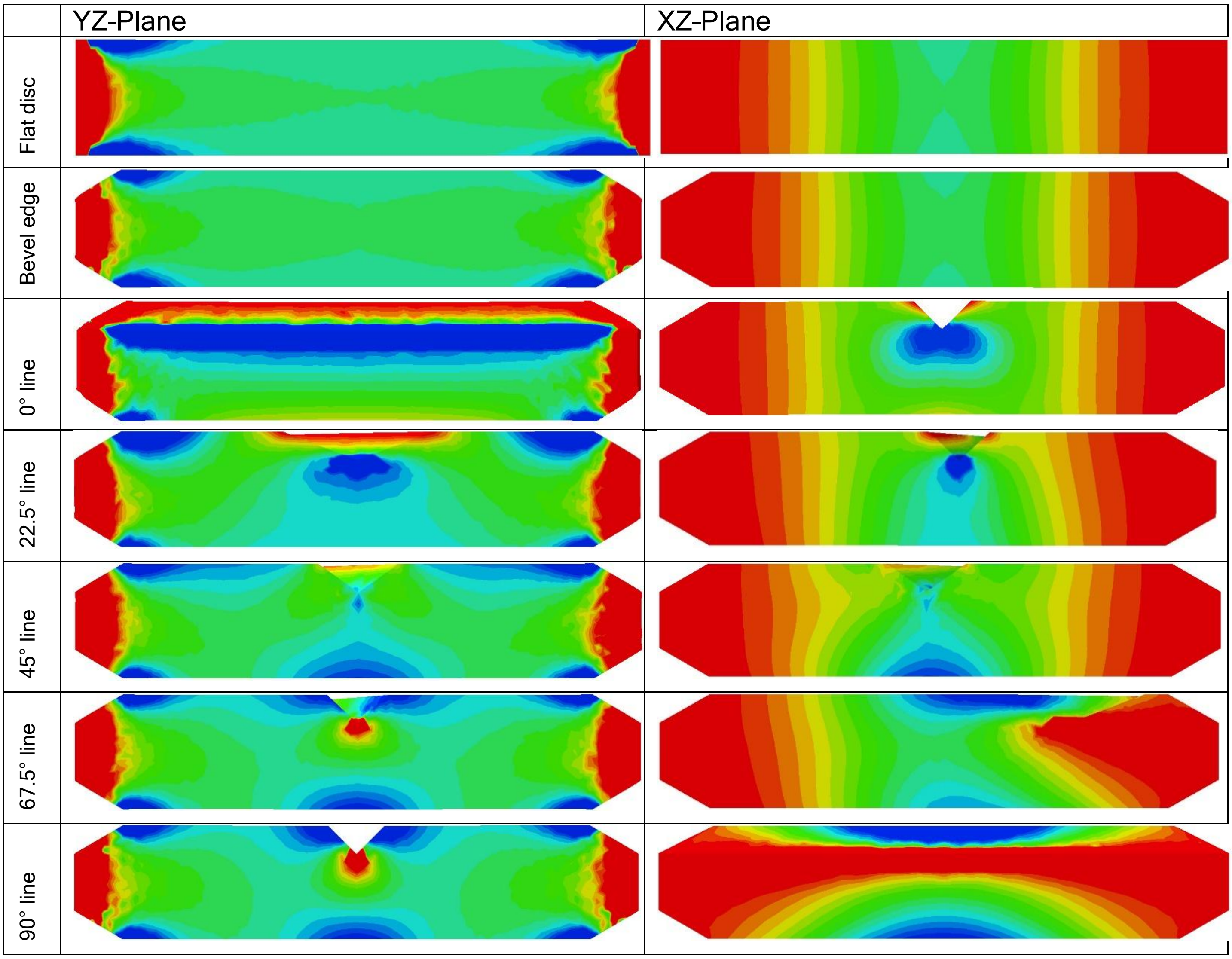

Figure 4: Normalised stresses across the z-axis, obtained on elastic discs (the solid line at a normalised stress of 1 represent the bevel-edged disc).

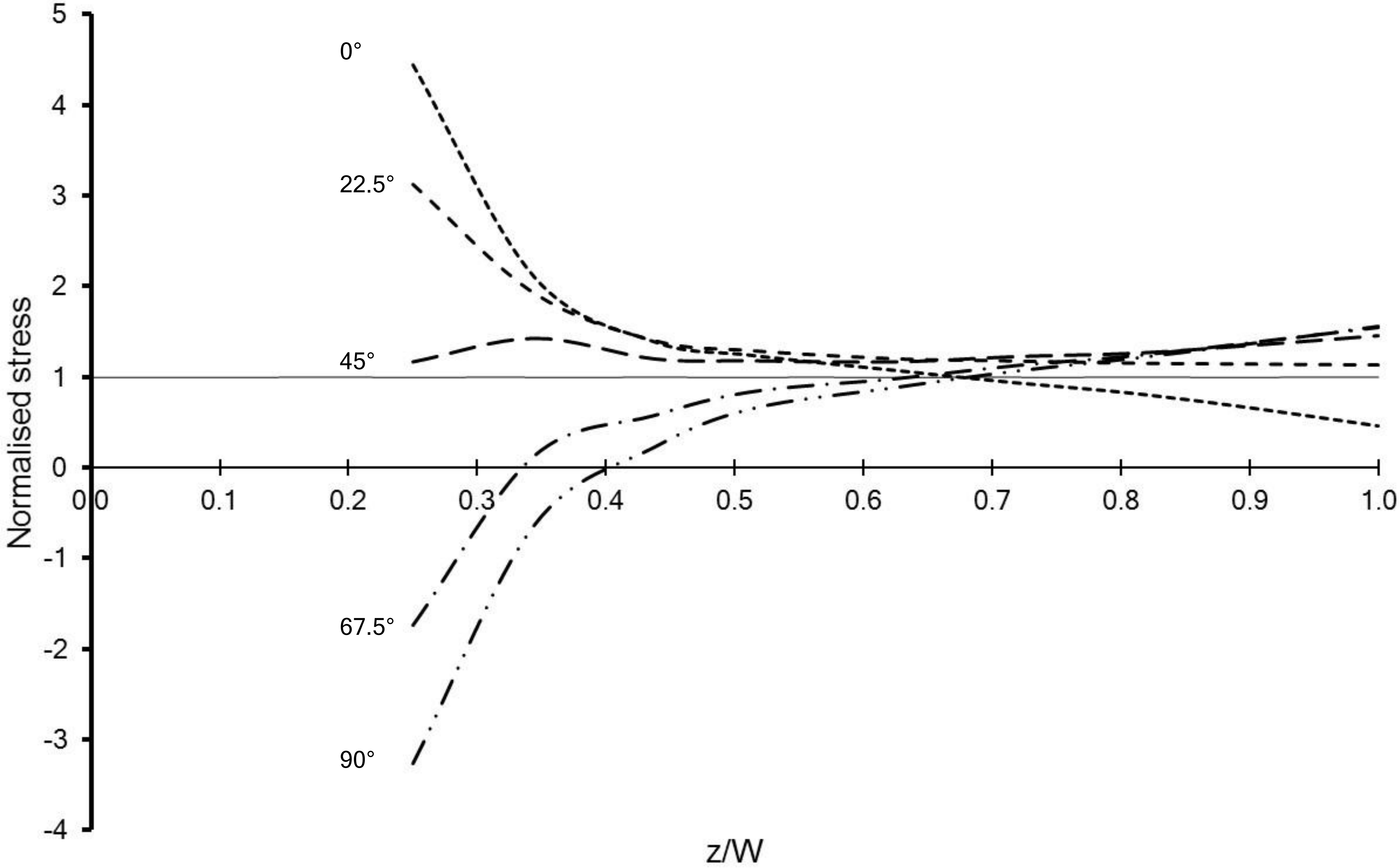

Figure 5

Maximum tensile stress as a function of the angle between the breaking line and the loaded diameter of the tablet.

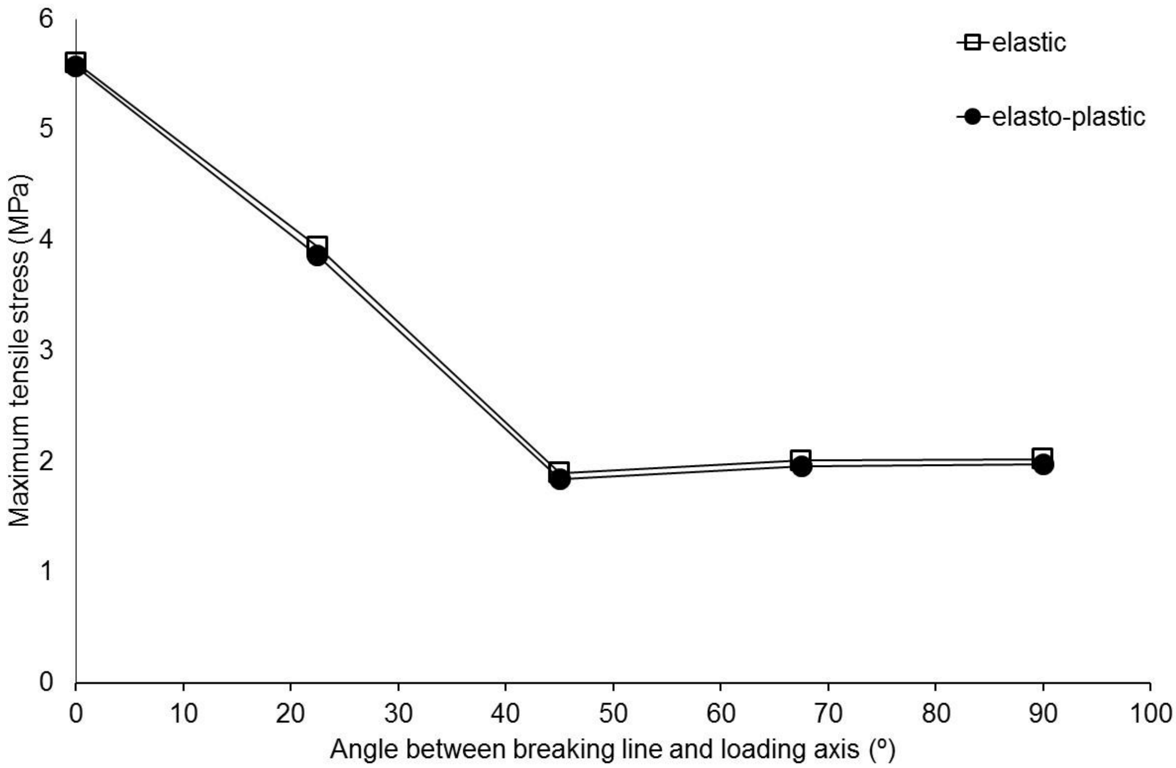

Figure 6a: Stress distribution in elasto-plastic discs with breaking line – XY-Plane.

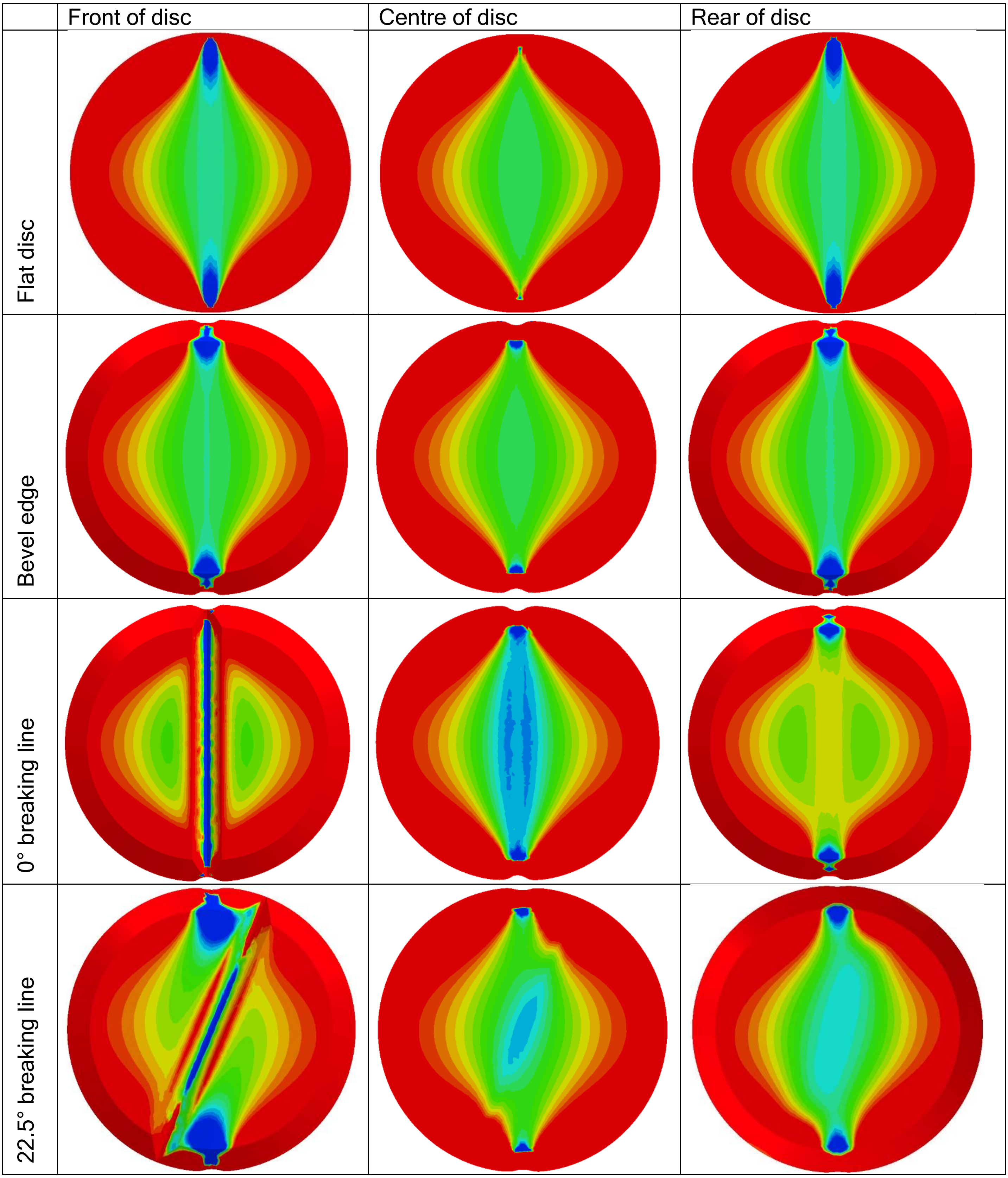

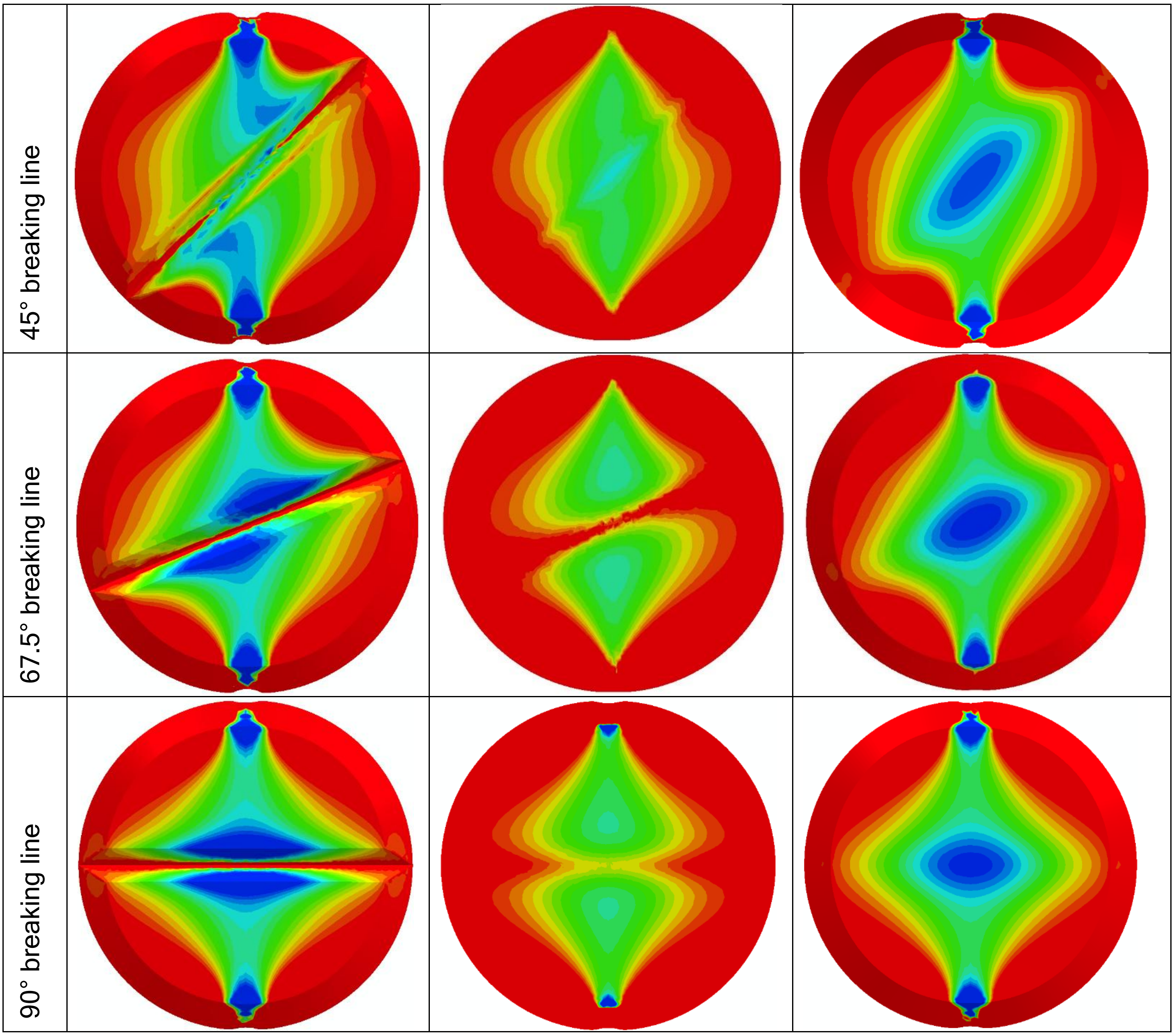

Figure 6a (continued)

Figure 6b: Stress distribution in elasto-plastic discs with breaking line – YZ and XZ-Planes.

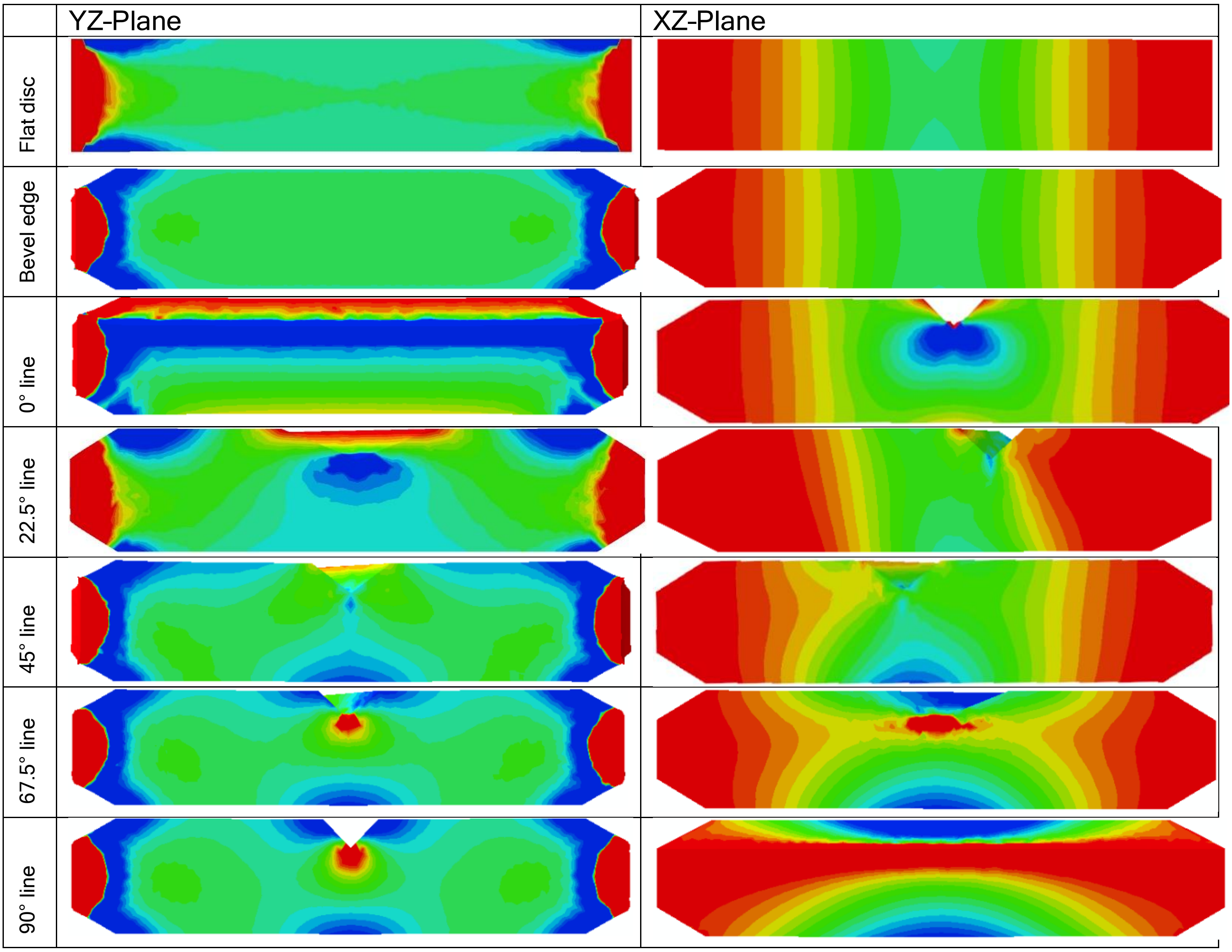

Figure 7: Normalised stresses across the z-axis, obtained on elasto-plastic discs (the solid line at a normalised stress of 1 represent the bevel-edged disc).

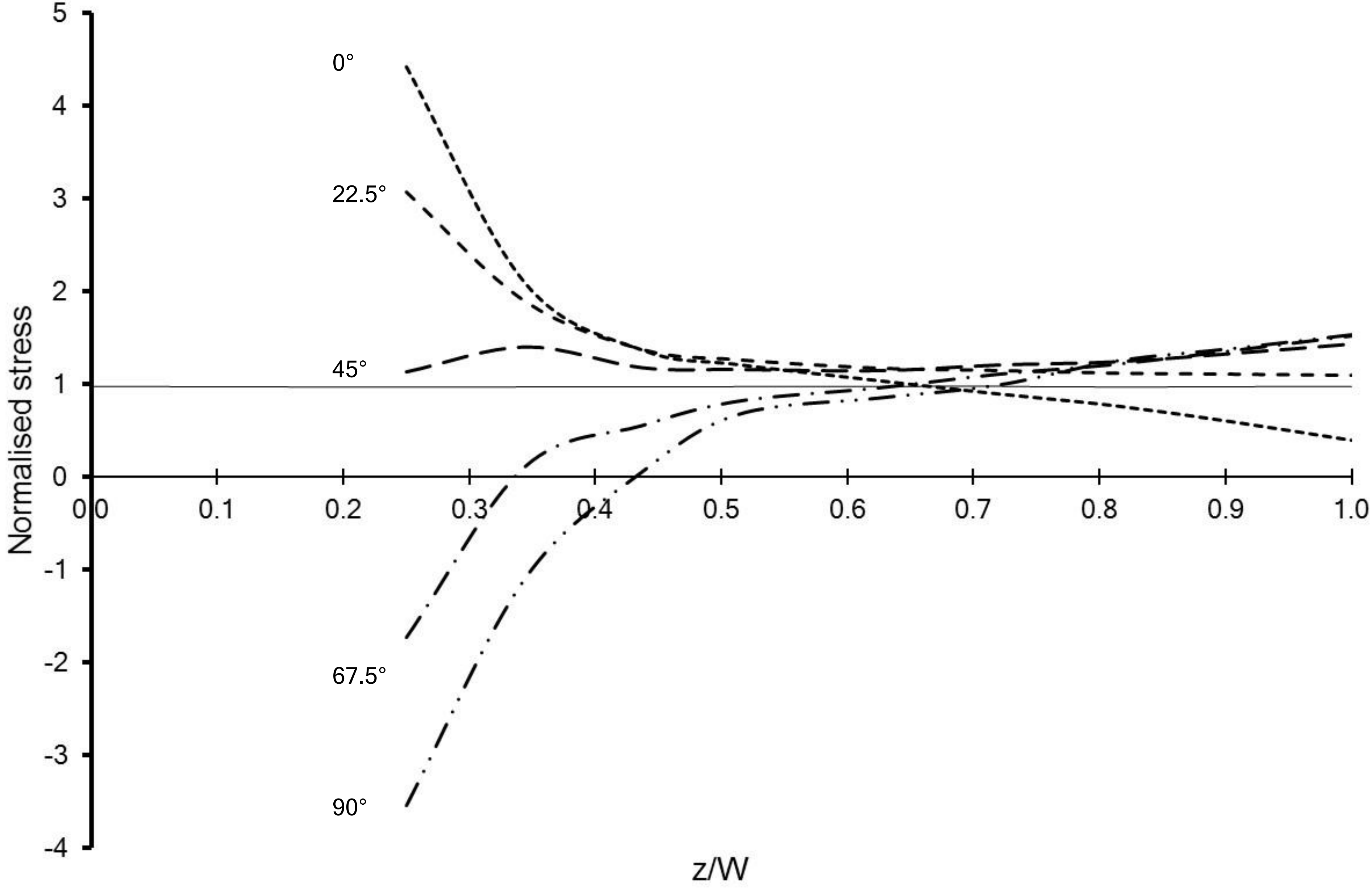

Figure 7b: Normalised von Mises stresses along the z-axis (coordinates *x=y=0*), comparing elastic (solid lines) and elasto-plastic (dashed lines) discs with a 90° angle between loading plane and breaking line (the lines at a normalised stress of 1 represent the bevel-edged discs).

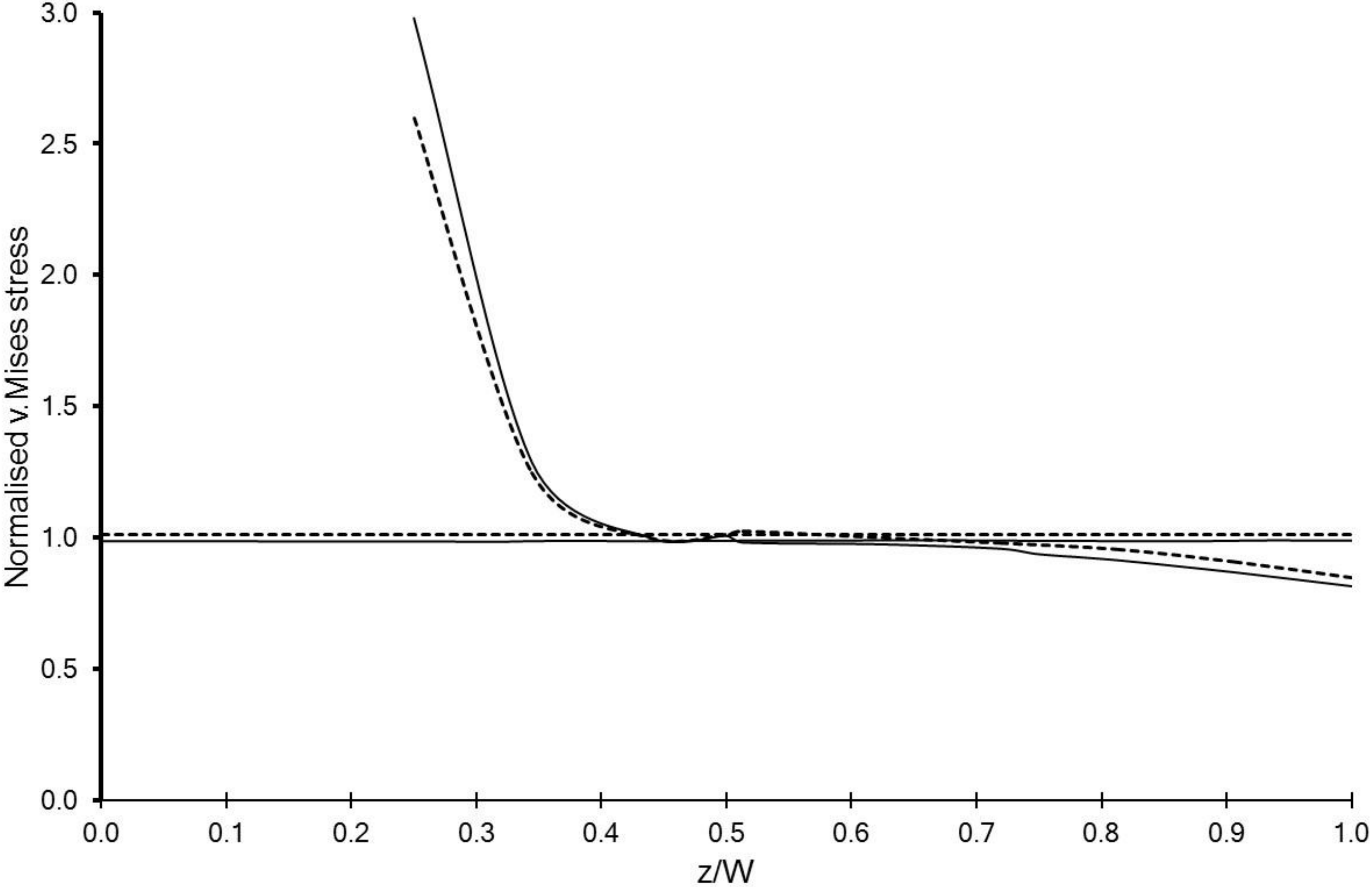

Figure 8

Crack initiation in Diarrhoea Relief Tablets, batch 4A058, at different breaking line positions relative to the loading diameter; (a) 0°; (b) 22.5°; (c) 45°; (d) 67.5°; (e) 90°.

(a)

(b)

(c)

(d)

(e)

Table 1

Tablet properties obtained on various commercially produced batches of tablets with a breaking line; [a]n = 10; [b]n = 30; [c]estimate; [d]n = 8; [e]n = 5; n.d. = not determined.

	Diarrhoea Relief Tablets		Aspirin Tablets
Tablet Property	B: 4A058	B: 3J114	B: 140032
Weight (mg)	801.2 ± 8.8[a]	810.3 ± 8.3[a]	598.0 ± 0.7[b]
Thickness W (mm)	3.661 ± 0.027[a]	3.612 ± 0.029[a]	3.427 ± 0.034[a]
Diameter D (mm)	12.813 ± 0.005[a]	12.808 ± 0.006[a]	12.788 ± 0.020[a]
W/D-ratio	0.286 ± 0.002[a]	0.282 ± 0.002[a]	0.268 ± 0.003[a]
Porosity[c] (%)	21.1 ± 0.3[a]	19.0 ± 0.3[a]	47.4 ± 0.6[a]
Breaking load (N) at a breaking line angle ϕ (see Fig. 1b) of:			
0°	51.5 ± 3.3[d]	63.1 ± 3.3[e]	63.2 ± 4.1[a]
22.5°	52.8 ± 5.3[d]	65.3 ± 2.1[e]	n.d.
45°	56.6 ± 3.0[d]	61.8 ± 2.7[e]	60.8 ± 4.4[a]
67.5°	55.6 ± 3.1[d]	61.5 ± 2.9[e]	n.d.
90°	52.7 ± 5.4[d]	61.9 ± 3.5[e]	63.7 ± 6.2[a]

Table 2

Comparison of maximum tensile stress values and centre tensile stress values of bevel-edged tablets with a breaking line, positioned at different angles to the loading plane, using different FEM-models. The “Factor” is the ratio between the considered angle ϕ (see Fig. 1b) and the 90° value.

FEM-Model	Angle	Stress (max) [MPa]	Factor	Centre stress [MPa]	Factor
Elastic	0°	5.605	2.8	1.638	3.0
	22.5°	3.942	2.0	1.679	3.1
	45°	1.896	0.9	1.480	2.7
	67.5°	2.009	1.0	0.880	1.6
	90°	2.021	(1.0)	0.540	(1.0)
Elasto-plastic	0°	5.568	2.8	1.603	2.9
	22.5°	3.868	2.0	1.641	3.0
	45°	1.844	0.9	1.442	2.6
	67.5°	1.955	1.0	0.845	1.5
	90°	1.978	(1.0)	0.551	(1.0)
Diarrhoea Relief Tablet	0°	4.287	2.8	1.324	1.3
	22.5°	3.644	2.4	1.323	1.3
	45°	1.882	1.2	1.286	1.2
	67.5°	1.508	1.0	1.122	1.1
	90°	1.519	(1.0)	1.034	(1.0)